Progress In Electromagnetics Research C, Vol. 30, 189–199, 2012

MEASUREMENT OF ELECTRICAL CHARACTERISTICS OF FEMALE BREAST TISSUES FOR THE DEVELOPMENT OF THE BREAST CANCER DETECTOR

T. H. Kim[1, *] and J. K. Pack[2]

[1]School of Information and Mechatronics, Gwangju Institute of Science and Technology, Gwangju, South Korea

[2]Department of Radio Science and Engineering, Chungnam National University, Daejeon, South Korea

Abstract—In this paper, dielectric characteristics of female breast tissues were measured. Breast Tissues were mainly composed of fat, fibro-glandular and tumor. Measured tissues were directly extracted from mice and a rat just before the measurements to maintain the tissues as fresh as living ones before degeneration. This makes the measured results more accurate. Because the extracted tissues were very thin, they were measured by two methods using HP probe and a newly designed two-port sample holder. Numerical results for the two-port sample holder were obtained for both the forward and inverse problems. Dielectric properties of breast tissues were measured in the frequency range between 50 MHz and 5 GHz. We calculated the electrical constant with the measured data from the two-port sample holder. As a result of the measurement, the dispersion characteristics of the female breast tissues were fitted into the first Cole-Cole model.

1. INTRODUCTION

Breast cancer is one of the most common cancers in women. One of the feasible methods to reduce breast cancer mortality is to detect tumors in their early stages, but computer tomography (CT) or magnetic resonance imaging (MRI) is very expensive. So X-ray mammography is currently the most effective imaging method for clinically detecting breast cancer. In X-ray tomography, a tissue is differentiated based on density. However, in most cases, tissue density does not depend on tissue physiological state. Important tissue

Received 7 May 2012, Accepted 4 June 2012, Scheduled 18 June 2012

* Corresponding author: Tae Hong Kim (thkim77@gist.ac.kr).

characteristics such as temperature, blood content, blood oxygenation and ischemia cannot be differentiated by X-ray tomography. So, the high false positive rate and high false negative rate are the limitations of the method. Also, X-ray mammography has drawbacks such as uncomfortable or painful breast compression and exposure to ionizing radiation. These drawbacks augment the search for techniques that image other physical tissue properties. Microwave imaging is one method that has been proposed to complement mammography. Tumor detection at microwave frequency is based on the significant contrast in dielectric properties between malignant tumors and normal fatty breast tissues. The dispersive characteristics of biological tissues depend on water content [1, 2]. A tumor's permittivity and conductivity are larger than those of a fatty tissue owing to more water content [3–5]. When exposed to microwaves, the high water content of malignant breast tumors cause significantly larger microwave scattering than normal fatty breast tissues with low water content. Active microwave imaging includes a radar using pulse signal and tomography using continuous wave or broadband signals. Radar type has the advantage of fast detection and simple measurement [6, 7]. Microwave tomography type has the advantage of dielectric property detection and identification [8, 9].

The purpose of this paper is to measure electrical characteristics of female human breast tissues — fatty, malignant and fibro-glandular, which will be used for the development of a detector for breast cancer. To measure the dielectric properties of female human breast tissues, we used a commercially available probe (Agilent co., HP85070B dielectric probe) [10] and a newly designed two-port sample holder. Dielectric properties of female human breast tissues — fatty, malignant and fibro-glandular tissues were measured in the frequency range from 50 MHz to 5 GHz using the open-ended coaxial probe and two-port sample holder system.

2. MEASUREMENT METHODS OF BROADBAND COMPLEX PERMITTIVITY

There are several methods for measuring the complex permittivity. Some of these methods for microwave frequency band need to measure reflection or transmission or both. The reflection method entails the measurement of reflection coefficients on the interface between two materials, on the open end of the coaxial line and the material being tested shown in Figure 1.

To calculate the complex permittivity from the measured reflection coefficient, it is useful to use an equivalent circuit of an open-

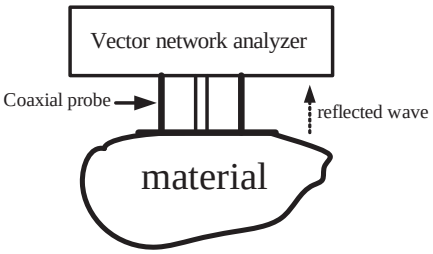

Figure 1. Open coaxial probe use for measuring complex permittivity of material.

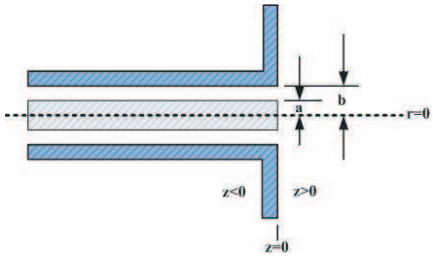

Figure 2. The structure of the open-ended coaxial probe.

ended coaxial line. The principle of the 1-port probe is as follows. Figure 2 shows the cross-section of the open-ended coaxial probe. The structure is composed of a center conductor with "a" radius and dielectric with "b" radius shown in Figure 2.

Open-ended coaxial transmission line probes are widely used as microwave sensors for industrial processes and quality control applications. In addition, they are used for measurement of the dielectric properties of materials. The admittance of the open-ended coaxial probe depends on the permittivity of the material under test, the radius of the probe, and the operating frequency [11, 12]. [13] has proved that flangeless cases provide adequate accuracy as long as the ratio of the outer conductor to the annular dielectric radius is at least 2 times the radius of the inner conductor. To estimate the complex permittivity of materials, we calculate the inverse scattering by using values of admittance of the open-ended coaxial line. Three different integral equations were compared by Xu et al. [14]. The equation by Levine et al. [15] is deemed appropriate for lossy dielectrics, which is of most interest:

$$Y = \frac{jk\varepsilon Y_0}{\log(b/a)\sqrt{\varepsilon_i}} \int_0^\infty \frac{d\zeta}{\zeta\sqrt{\zeta^2 - k^2\varepsilon}} \left[J_0(\zeta a) - J_0(\zeta b)\right]^2 \tag{1}$$

where Y_0 is the characteristic impedance of the coaxial line, $\varepsilon = \varepsilon_r' - j\varepsilon_r''$ the complex dielectric permittivity of the material, ε_i the permittivity of the coaxial line's filling material, ζ the integral variable, k the wave number, and J_0 a first-type Bessel function of zero order.

Admittance Y is related to the measured reflection coefficient

$$Y = Y_0 \frac{1 - \Gamma}{1 + \Gamma} \tag{2}$$

where Γ and Y_0 are the measured reflection coefficient and characteristic admittance of the probe.

The advantage of the open-ended coaxial probe is broad-band measurement and no necessity to prepare a sample of a specific size, as long as the sample meets the minimum size requirements. But it has limitations in the requirement of sample shape, size, consistency, and placement. As for shape, the sample needs to be thick enough so that all the available fields in the vicinity of the probe are located inside the material. For the best accuracy, having the material thickness four times the aperture diameter is recommended [10].

Figure 3 shows the commercial probe for dielectric measurement. Table 1 and Figure 3 shows the general characteristics of the HP 85070B dielectric probe.

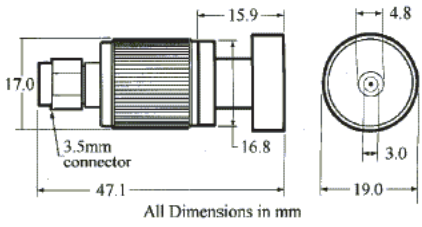

Figure 3. HP 85070B dielectric probe.

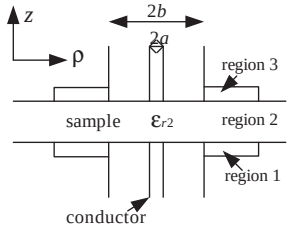

Figure 4. Structure of two-port sample holder.

Table 1. The characteristics of the HP 85070B dielectric probe.

		Characteristics
Frequency range		200 MHz $\sim$ 20 GHz $\left(f_{\max} = \frac{110\,GHz}{\sqrt{\lvert\varepsilon_r^*\rvert}}\right)$
Temperature range		$-40°\mathrm{C} \sim 200°\mathrm{C}$
Temperature rate		$< 10°\mathrm{C}$ per minute
accuracy	Dielectric constant	$\pm 5\%$
	loss tangent	$\pm 0.05\%$
maximum dielectric constant		<100
minimum lose tangent		>0.05
permeability		$\mu_r = 1$
flatness		< 25 mm
diameter		>20 mm
thickness		$> \frac{20mm}{\sqrt{\lvert\varepsilon_r^*\rvert}}$

If the material is very thin, the measurement of the open-ended coaxial probe is less accurate. So, the two-port measurement method using both the transmission and reflection coefficients is needed. Figure 4 shows a sectional drawing of the two-port coaxial sample holder. The sample holder allows a measurement of the insertion and return losses of a thin material as a function of frequency. It will be assumed that the coaxial line operates at a frequency so that only the fundamental TEM mode is propagating. Evanescent TM_{0n} modes are also assumed to exist in the coaxial line near the probe ends [16]. The azimuthally symmetric H_ϕ mode in the coaxial line induces a H_ϕ magnetic field in the homogeneous and isotropic material under test.

Equation (3) is the Helmholtz' equation.

$$\left[\frac{\partial^2}{\partial\rho^2}+\frac{1}{\rho}\frac{\partial}{\partial\rho}-\frac{1}{\rho^2}+\frac{\partial^2}{\partial z^2}+k_i^2\right]H_{\phi i}(\rho,z)=0 \tag{3}$$

For an incident wave travelling in the lower coaxial line, the radial component of the normalized solution in the coaxial line is a linear combination of TEM and TM_{0n} modes of Equations (4)–(6).

$$E_{\rho 1}(\rho,z)=R_0(\rho)e^{-\gamma_0 z}+\sum_{m=0}^{\infty}S_{11(m)}R_m(\rho)e^{\gamma_{m(c)}z},\quad \rho\in[a,b] \tag{4}$$

$$E_{\rho 2}(\rho,z)=\int_0^\infty \zeta J_1(\zeta\rho)\frac{\gamma_2}{j\omega\varepsilon_2^*}\{A(\zeta)e^{-\gamma_2(z-d)}-B(\zeta)e^{\gamma_2(z-d)}\}d\zeta,$$
$$\rho\in[0,\infty] \tag{5}$$

$$E_{\rho 3}(\rho,z)=\sum_m S_{21(m)}R_m(\rho)e^{-\gamma_{m(c)}(z-d)},\quad \rho\in[a,b] \tag{6}$$

The scattering parameters may be constructed if we match at interfaces the Hankel transforms of the Equations (4)–(6) and analogous equations for the magnetic field, solve for coefficients, and then take inverse transforms. The result is given in the following two independent vector relations:

$$Q_1\overrightarrow{S_{11}}+Q_2\overrightarrow{S_{21}}=\overrightarrow{P_1} \tag{7}$$

$$Q_2\overrightarrow{S_{11}}+Q_1\overrightarrow{S_{21}}=\overrightarrow{P_2} \tag{8}$$

where the components of the matrices are given by

$$Q_{1mn}=\frac{\delta_{mn}}{\gamma_{n(c)}}+\frac{\varepsilon_2^*}{\varepsilon_c^*}\int_0^\infty\frac{\zeta D_nD_m[\exp(2\gamma_2 d)+1]}{\gamma_2[\exp(2\gamma_2 d)-1]}d\zeta \tag{9}$$

$$Q_{2mn}=-2\frac{\varepsilon_2^*}{\varepsilon_c^*}\int_0^\infty\frac{\zeta D_nD_m\exp(2\gamma_2 d)}{\gamma_2[\exp(2\gamma_2 d)-1]}d\zeta \tag{10}$$

$$P_{1m}=\frac{\delta_{m0}}{\gamma_{n(c)}}-\frac{\varepsilon_2^*}{\varepsilon_c^*}\int_0^\infty\frac{\zeta D_mD_0[\exp(2\gamma_2 d)+1]}{\gamma_2[\exp(2\gamma_2 d)-1]}d\zeta \tag{11}$$

$$P_{2m} = \frac{\varepsilon_2^*}{\varepsilon_c^*} \int_0^\infty \frac{\zeta D_0 D_m \zeta \exp(\gamma_2 d)}{\gamma_2[\exp(2\gamma_2 d) - 1]} d\zeta \tag{12}$$

Straightforward matrix manipulation of Equations (7) and (8), assuming that no singular matrix inverses are encountered, yields the following solution for the forward problem.

$$\overrightarrow{S_{21}} = [Q_1 - Q_2 Q_1^{-1} Q_2]^{-1} (\vec{P}_2 - Q_2 Q_1^{-1} \vec{P}_1) \tag{13}$$

$$\overrightarrow{S_{11}} = Q_1^{-1} (\vec{P}_1 - Q_2 \vec{S}_{21}) \tag{14}$$

Figure 5 shows the flowchart for calculating complex permittivity using a two-port sample holder. To solve the inverse problem, we used a direct search algorithm as the optimization algorithm.

3. MEASUREMENT AND FITTING OF FEMALE BREAST TISSUES

In this paper, dispersive characteristics for fatty, malignant and fibro-glandular biological tissues of were measured. Fat and fibro-glandular tissues were extracted from a pregnant rat and breast-feeding mice,

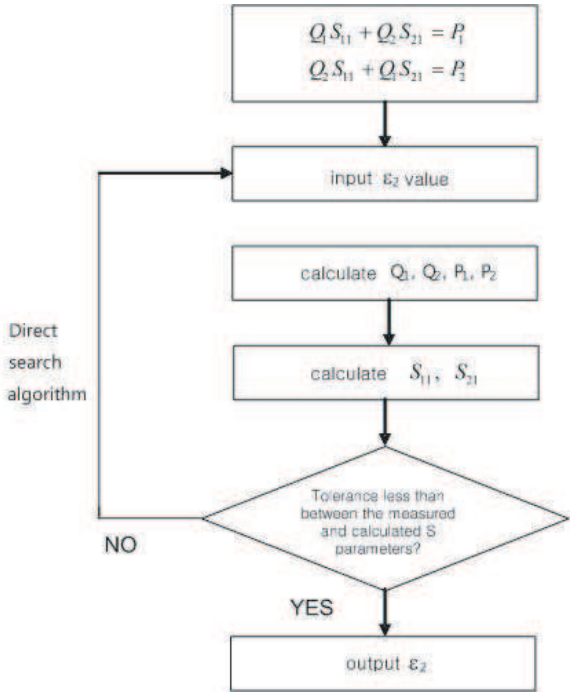

Figure 5. Flowchart for calculating complex permittivity using two-port measurement.

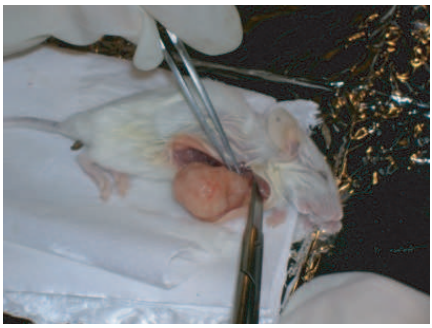

Figure 6. Picture extracting the tumor from a mouse.

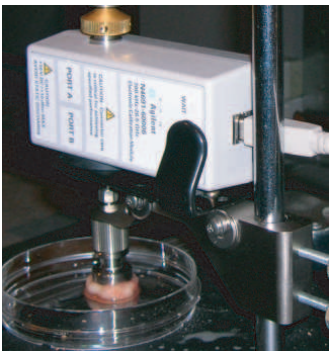

Figure 7. Measurement of the breast cancer tissue using the HP probe.

Figure 8. Fabricated sample holder.

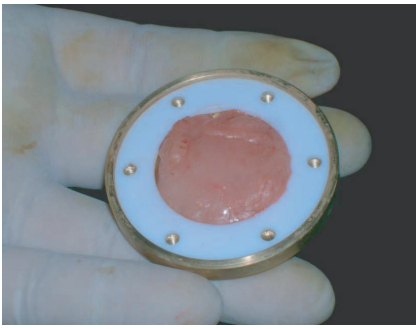

Figure 9. Breast tissue in two-port sample holder.

respectively. And the tumor for the breast cancer was cultivated using the xenograft method and extracted. Tissues were extracted from the mice and rat just before the measurements to maintain freshness. This makes the measured values more accurate. Figure 6 shows a picture of extracting the tumor from a mouse.

We measured the extracted tissues by two methods. First, the complex permittivities of tissues are calculated from the reflection signals measured by the vector network analyzer (VNA) and HP probe. The probe is connected to the VNA through a high-quality flexible cable. Figure 7 shows the measurement of the complex permittivities using the HP open-coaxial probe. The extracted tissues are very thin and not enough to be measured by the HP probe.

Secondly, we measured the reflection and transmission of those using the newly designed two-port sample holder and VNA. Figure 8 shows the newly fabricated sample holder. The specimen has a size with 30 mm diameter and 1.5 mm thickness.

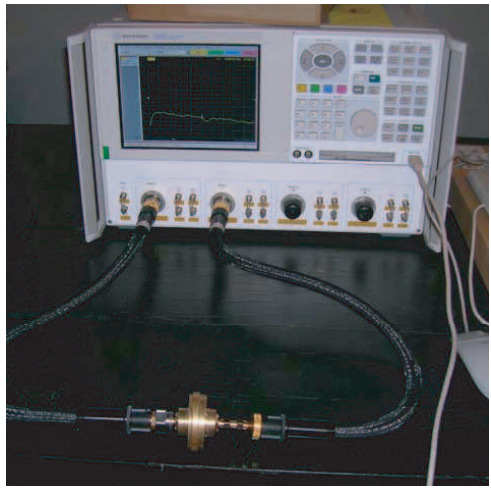

Figure 10. Measurement of the breast cancer tissue using two-port sample holder.

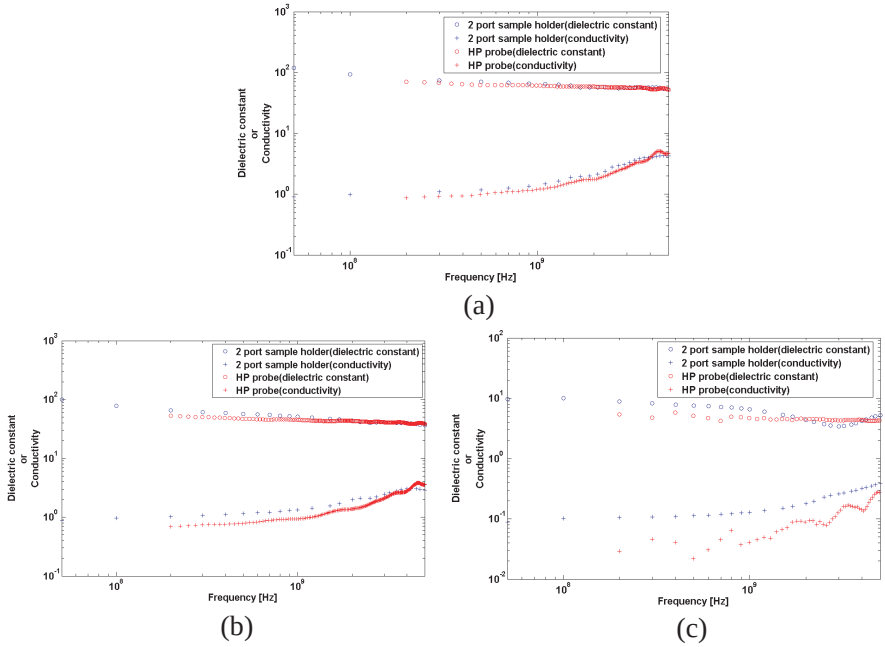

Figure 11. Comparisons of the measured results. (a) Fat. (b) Fibroglandular. (c) Tumor.

Figure 9 shows the extracted cancerous tissue from the mouse, and Figure 10 represents the measurement using sample holder and VNA.

The measured complex permittivities of fat, fibro-glandular, and breast cancer samples are shown in Figure 11. We measured with the HP probe from 200 MHz to 5 GHz and two-port sample holder from 50 MHz to 5 GHz in the frequency band.

The two measured results of HP probe and two-port sample holder are quite similar in the high frequency band. As the measured tissues are thin, there are differences in the low frequency band and in the fat tissue. Due to metal losses of the coaxial line itself, the open-ended coaxial probe is not accurate for the characterization of the dielectric loss factor for very low loss dielectric sample such as fat tissue. So, we made the fitting by the first Cole-Cole model of Equation (15) with measured results from the two-port sample holder.

$$\varepsilon(\omega) = \varepsilon_\infty + \frac{\varepsilon_s - \varepsilon_\infty}{1 + (j\omega\tau)^{1-\alpha}} + \frac{\sigma}{j\omega\varepsilon_0} \tag{15}$$

where ω is the angular frequency, $\varepsilon(\omega)$ the complex permittivity, ε_∞ the high frequency permittivity, ε_s the static permittivity, τ the relaxation time constant, α the parameter that allows for the broadening of the dispersion, and σ the static conductivity.

Table 2. The 1st Cole-Cole parameters of the female breast tissues.

Tissue Type	ε_s	ε_∞	τ [ps]	α	σ
Tumor	4	91.68	23.42	0.6106	0.8985
Fibro-glandular	2.5	76.31	35.10	0.6087	0.8825
Fat	2.5	8.74	99.73	0.2055	0.0879

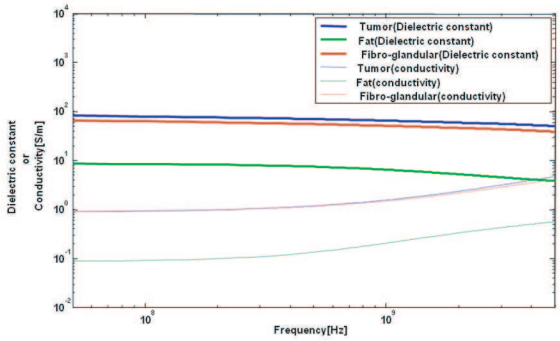

Figure 12. Comparison of the fitted results with the 1st Cole-Cole model

Figure 12 represents dispersive characteristics of breast tissues using the first Cole-Cole model. Breast cancer tissue showed quite different dispersion characteristics from normal tissue. But malignant tissue showed little difference from fibro-glandular tissue.

4. CONCLUSIONS

Dispersive characteristics of fatty, malignant and fibro-glandular tissues for female breast were measured and analyzed in this paper, which will be used for the development of a detector for breast cancer. Since the tissues were extracted from the mouse just before the measurements, they were maintained as fresh as living tissues in the measurements. Dielectric properties of fatty, malignant and fibro-glandular tissues were measured using a one-port open-ended coaxial probe and a two-port sample holder. Because extracted tissues were very thin, they were measured by two methods using the HP probe and the newly designed two-port sample holder. Dielectric properties of breast tissues were measured in the frequency range between 50 MHz and 5 GHz. Numerical results for the two-port sample holder are obtained for both the forward and inverse problems. We calculated the electrical constant with the measured data from the two-port sample holder. As a result of the measurement, the dispersion characteristics of the female breast tissues were fitted into the first Cole-Cole model.

REFERENCES

1. Gabriel, S., R. W. Law, and C. Gabriel, "The dielectric properties of biological tissue: III. Parametric models for the dielectric spectrum of tissues," *Phys. Med. Biol.*, Vol. 14, 2271–2293, 1996.
2. Vorst, V., A. Rosen, and Y. Kotsuka, *RF/Microwave Interaction with Biological Tissues,* Wiley, Hoboken, NJ, 2006.
3. Joines, W. T., Y. Zhang, C. Li, and L. Jirtle, "The measured electrical properties of normal and malignant human tissues from 50 to 900 MHz," *Med. Phys.*, Vol. 21, No. 4, 547–550, 1994.
4. Surowiec, A. J., S. S. Stuchly, J. R. Barr, and A. Swarup, "Dielectric properties of breast carcinoma and the surrounding tissues," *IEEE Trans. Biomed. Eng.*, Vol. 35, No. 4, 257–263, 1988.
5. Forster, K. R. and J. L. Schepps, "Dielectric properties of tumor and normal tissues at radio through microwave frequencies," *J. Microwave Power*, Vol. 16, No. 2, 47–54, 2001.
6. Chen, Y., I. J. Craddock, and P. Kosmas, "Feasibility study of lesion classification via contrast-agent-aided UWB breast

imaging," *IEEE Trans. Biomed. Eng.*, Vol. 57, No. 5, 1003–1007, May 2010.

7. Mashal, A., B. Sitharaman, L. Xu, P. K. Avti, A. V. Sahakian, J. H. Booske, and S. C. Hagness, "Toward carbon-nanotube-based theranostic agents for microwave detection and treatment of breast cancer: Enhanced dielectric and heating response of tissue mimicking materials," *IEEE Trans. Biomed. Eng.*, Vol. 57, No. 8, 1831–1834, Aug. 2010.
8. Meaney, P. M., M. W. Fanning, T. Raynolds, C. J. Fox, Q. Fang, C. A. Kogel, S. P. Poplack, and K. D. Paulsen, "Initial clinical experience with microwave breast imaging in women with normal mammography," *Acad. Radiol.*, Vol. 14, No. 2, 207–218, Feb. 2007.
9. Pedersen, P. C., C. C. Johnson, C. H. Durney, and D. G. Bragg, "Microwave reflection and transmission measurements for pulmonary diagnosis and monitoring," *IEEE Trans. Biomed. Eng.*, Vol. 25, No. 1, 40–48, Jan. 1978.
10. Blackham, D. V. and R. D. Pollard, "An improved technique for permittivity measurements using a coaxial probe," *IEEE Trans. Instrum. Meas.*, Vol. 46, No. 5, 1093–1099, 1997.
11. http://cp.literature.agilent.com/litweb/pdf/5091-6247EUS.pdf.
12. Misra, D., "A quasistatic analysis of open-ended coaxial lines," *IEEE Transactions on Microwave Theory and Techniques*, Vol. 35, No. 10, 925–928, 1987.
13. McLaughlin, B. L., et al., "Miniature open-ended coaxial probes for dielectric spectroscopy applications," *J. Phys. D: Appl. Phys.*, Vol. 40, 45–53, 2007.
14. Xu, Y., et al., "Some calculation methods and universal diagrams for measurement of dielectric constants using open-ended coaxial probes," *IEE Proc.-H*, Vol. 138, No. 4, 1991.
15. Levine, H. R., et al., "Theory of the circular diffraction antenna," *J. Appl. Phys.*, Vol. 22 29–43, 1951.
16. Jarvis, J. B. and M. D. Janezic, "Analysis of a two-port flanged coaxial holder for shielding effectiveness and dielectric measurements of thin films and thin materials," *IEEE Trans. Electromag. Compat.*, Vol. 38, No. 1, 67–70, 1996.